Environmental Science and Pollution Research (2018) 25:5902–5910
https://doi.org/10.1007/s11356-017-0943-9

RESEARCH ARTICLE

Catalytic degradation of sulfaquinoxalinum by polyester/poly-4-vinylpyridine nanofibers-supported iron phthalocyanine

Nan Li[1] · Panting Lu[1] · Cuixia He[1] · Wangyang Lu[1] · Wenxing Chen[1]

Received: 29 July 2017 / Accepted: 4 December 2017 / Published online: 12 December 2017

Abstract

Iron (II) phthalocyanine (FePc) supported on electrospun polyester/poly-4-vinylpyridine nanofibers (PET/P4VP NFs) was prepared by stirring in tetrahydrofuran. The resulting product was confirmed and characterized by ultraviolet-visible diffuse reflectance spectroscopy, attenuated total reflection Fourier transform infrared spectra, X-ray photoelectron spectroscopy, gas chromatography/mass spectrometry, and ultra-performance liquid chromatography. More than 95% of sulfaquinoxalinum (SQX) could be removed by the activation of hydrogen peroxide in the presence of FePc-P4VP/PET with a PET and P4VP mass ratio of 1:1. This system exhibited a high catalytic activity across a wide pH and temperature range. The degradation rates of SQX achieved 100, 95, and 78% at a pH of 3, 7, and 9, respectively, and the degradation rates of SQX are more than 80% at the temperature ranging from 35 to 65 °C. $DMSO_2$ could be detected by gas chromatography/mass spectrometry after the addition of DMSO, suggesting the formation of the high-valent iron intermediates in this catalytic system. In addition, the electron paramagnetic resonance experiments proved that free radicals did not dominate the reaction in our system. Therefore, the high-valent iron intermediates were proposed to the main active species in the FePc-P4VP/PET/hydrogen peroxide system. In summary, the heterogeneous catalytic processes with non-radical catalytic mechanism might have better catalytic performance for the removal of organic pollutants, which can potentially be used in wastewater treatment.

Keywords Iron (II) phthalocyanine · Nanofiber · Sulfaquinoxalinum · Hydrogen peroxide · Catalytic oxidation · Free radical · High-valent iron intermediate

Introduction

Pharmaceutical antibiotics have been used widely in recent decades (Wang et al. 2012; Wang et al. 2013; Hoff et al. 2014; Biošić et al. 2017) and have become the subject of growing attention as soil environmental contaminants (Bloem et al. 2017; Yu et al. 2013; Carmona et al. 2014; Hou et al. 2016; Kovacic et al. 2016). Discharged antibiotics can enter the aqueous environment from soil and sediments by surface runoff, leaching, and desorption (Lekunberri et al. 2017; Kay et al. 2005) and eventually flow into drinking water. Sulfonamides (SAs), as one of the most important and widely used antibiotics (Zhao et al. 2017; Lin et al. 2017; Ben et al. 2017; Bialk-Bielinska et al. 2011; Zhang et al. 2013; Ou et al. 2015), are synthetic antimicrobials derived from sulfanilic acid (Guo et al. 2012a). Significant residual amounts of sulfonamides have been detected, including in rivers, groundwater, and soil, especially in wastewater from animal farms and hospitals (Sakai et al. 2016; Baran et al. 2011). Sulfaquinoxaline (SQX) was one of the first compounds that was introduced to prevent and treat coccidia (Hoff et al. 2009, 2014). SQX consists of a sulfa group and a quinoxaline group (Hoff et al. 2012). It has been reported that sulfas do not show high toxicities to larger organisms and

Responsible editor: Suresh Pillai

Electronic supplementary material The online version of this article (https://doi.org/10.1007/s11356-017-0943-9) contains supplementary material, which is available to authorized users.

✉ Wangyang Lu
luwy@zstu.edu.cn

[1] National Engineering Laboratory for Textile Fiber Materials & Processing Technology (Zhejiang), Zhejiang Sci-Tech University, Hangzhou 310018, China

human beings; however, quinoxaline exhibits mutagenic and carcinogenic activities (Liao et al. 2016). Methodologies for SQX removal from contaminated environments encompass physical, chemical (Guo et al. 2012b) and biological (Vasiliadou et al. 2013; Cetecioglu 2014) techniques. Advanced oxidation processes (AOPs) have been considered to be efficient and environmentally friendly methods (Mantzavinos et al. 2014, 2017; Dewil et al. 2017) to decompose various robust microorganic contaminants in surface water and wastewater into less complex and less harmful by-products (Salaeh et al. 2016); some of these methods can even mineralize contaminants into carbon dioxide, water, and other inorganics (González et al. 2013; Mano et al. 2015; Wols et al. 2015). However, AOP degradation was carried out by hydroxyl radicals (·OH) (Wang et al. 2017; Wang et al. 2013; Liu and Wang 2013).

In our previous studies (Zhu et al. 2016), to prevent the formation of dimers and oligomers, the degradation of carbamazepine and Rhodamine B was investigated during a Fenton-like process (Nidheesh et al. 2013, Nidheesh and Gandhimathi 2014a, b) with iron (II) phthalocyanine (FePc)/polyacrylonitrile nanofibers in which FePc molecules were isolated in polyacrylonitrile nanofibers by electrospinning. Methods for preparing a supported catalyst by phthalocyanine have been provided (Sorokin and Kudrik 2011; Sorokin 2013): (i) physical adsorption onto a support surface, (ii) encapsulation within porous materials, (iii) electrostatic force between oppositely charged complexes and surface, (iv) grafting via direct coordination of metal to a support, and (v) covalent anchoring to a support.

Since the nitrogen atoms can coordinate axially with iron phthalocyanine in the center of metallic iron, we can obtain structurally stable complexes. At the same time, this method can avoid the formation of dimers and oligomers of iron phthalocyanine to improve its catalytic activity. Furthermore, the heterogeneous catalyst can be prepared by using polyester as a carrier to avoid the secondary pollution of water resources. The aim of our work was to study whether active species of Fe(IV) = O are produced by grafting via direct metal coordination. In this study, polyester (PET)-supported poly-4-vinylpyridine (P4VP) nanofibers were prepared by electrospinning; whereafter, the FePc was modified by using the PET/P4VP nanofibers to prepare the catalysts. The catalyst was analyzed by attenuated total reflection Fourier transform infrared spectroscopy (ATR-FTIR), ultraviolet-visible diffuse reflectance spectroscopy (UV-vis), and X-ray photoemission spectroscopy (XPS). Sulfaquinoxaline (SQX) was the main organic substance used to investigate catalytic activity. The possible formations of reactive species were examined by using isopropanol (IPA), 5,5-dimethyl-pyrroline-oxide (DMPO) spin trapping, electron paramagnetic resonance (EPR), and dimethyl sulfoxide (DMSO).

Materials and methods

Materials

FePc and the spin trapping reagent, DMPO were purchased from Tokyo Chemical Industry Co., Ltd. (Tokyo, Japan). Hydrogen peroxide (H_2O_2, 9.7 M) was supplied from Sinopharm Chemical Reagent Co., Ltd. (Tianjin, China). Polyethylene terephthalate (PET) chips were obtained from Jiangsu Hengli Chemical Fibre Co., Ltd. (Jiangsu, China). P4VP, SQX, and other sulfonamides (SAs) were supplied from J&K Chemical Inc. (Beijing, China). IPA and DMSO were purchased from Tianjin Wing Tai Chemical Co., Ltd. (Tianjin, China). Tetrahydrofuran (THF) and hexafluoroisopropanol (HFIP) were obtained from Tianjin Yongda Chemical Reagent Co., Ltd. (Tianjin, China). Chemicals and solvents were all of analytical grade and used without any further purification. In all experiments, the ultrapure water was obtained from Milli-Q Advantage A10 (Millipore).

Preparation of FePc-P4VP/PET

PET chips and P4VP (12 wt% PET and P4VP vs. HFIP) were dissolved in HFIP with PET and P4VP mass ratios of 10:1, 5:1, and 1:1, respectively. After the solution had been mixed at room temperature for 12 h, PET/P4VP was added to a syringe that was equipped with a metal spinneret in the electrospinning apparatus. The PET/P4VP solutions were electrospun at 15 kV. The electrospun PET/P4VP nanofibers were deposited onto a grounded tinfoil sheet, where the tip-to-collector distance was fixed at 18 cm and the volumetric flow rate was 1 mL/h. Spinning was conducted under a relative humidity of 60%. After electrospinning, PET/P4VP was removed from the tinfoil sheet and was cut almost to the size of a sheet. These nanofiber sheets were added to the THF solution of the FePc in a three-necked flask container. The three-necked flask was heated and stirred at 70 °C in a water bath. After 12 h, the reactant was removed from the solution, rinsed with THF and distilled water many times to remove unreacted FePc and other residuals, and freeze dried in vacuum to constant weight. The reaction course is indicated in Scheme 1.

Characterization

The FePc content in FePc-P4VP/PET was measured by UV-vis spectrophotometry (UV-2550, Shimadzu, Japan). Iron phthalocyanine powder was added into a HFIP solution at a series of concentrations; the absorbance was measured and an absorbance–concentration standard curve was produced. A certain amount of FePc-P4VP/PET was weighed into the HFIP solution; the absorbance was measured and the FePc content was determined. The chemical structure of the FePc powders, PET NFs, FePc/PET NFs, FePc-P4VP NFs, and

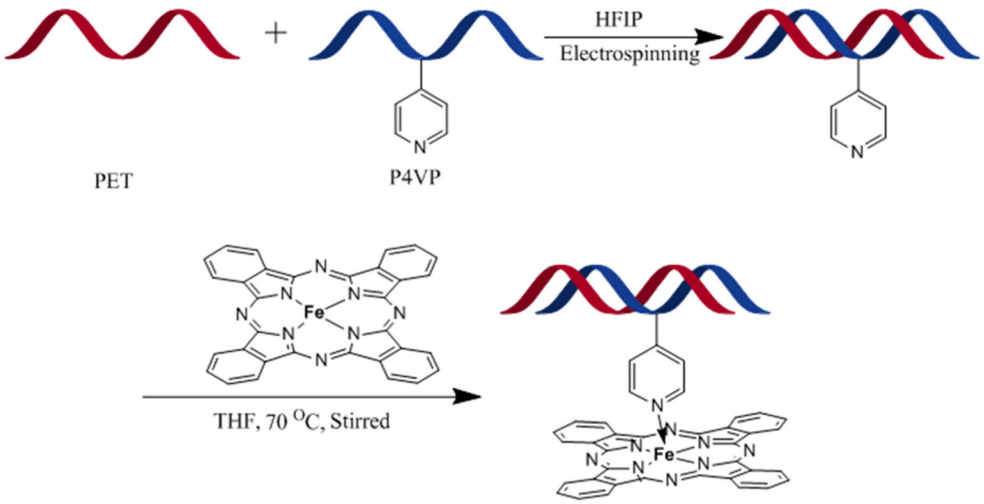

Scheme 1 Preparation of FePc-P4VP/PET

FePc-P4VP/PET was analyzed by ATR-FTIR spectra (Nicolet 5700, Perkin Elmer, USA) and UV-vis, and XPS (Kratos AXIS Ultra DLD, Kratos, UK) data were recorded with a Thermo Scientific K-Alpha spectrometer (monochromatic Al Ka, 1486.6 eV).

Degradation experiments

The degradation of SQX and other SAs was carried out in a 40-mL glass sample beaker, with a reaction temperature of 50 °C (or other temperatures as desired) using a constant temperature shaker water bath (DSHZ 300A, Taicang, Jiangsu). FePc-P4VP/PET (40 mg) was added to 20 mL SQX (0.02 mM) or other aqueous solution of SAs (0.02 mM) with H_2O_2 (10 mM) as oxidant. The solution pH was adjusted by H_2SO_4 or NaOH addition. The evolution of SQX and other sulfa antibiotic concentrations was monitored by ultra-performance liquid chromatography-UV (Waters, USA) equipped with a Waters BEH-C18 column.

EPR study

EPR signals were detected on a Bruker A300 spectrometer for free radicals trapped by DMPO in aqueous or in methanol solution. Typical parameter settings were the following: center field, 3507 G; sweep width, 80 G; static field, 3467.5 G; microwave frequency, 9.85 GHz; and modulation frequency, 100 kHz. EPR signals of FePc-P4VP/PET that contains 10 mM DMPO were observed after 100-s reaction in the presence of H_2O_2.

Ferric detection experiments

Experiments for detecting high-valent iron intermediates were carried out as follows. FePc-P4VP/PET (40 mg) and FePc/PET NFs (40 mg) were dispersed in 20 mL DMSO aqueous solution (10 mM) and compared with a control group (DMSO solution only). The solution was stirred continuously for 120 min after 10 mM H_2O_2 injection. Products were extracted by rotary evaporation and were redissolved with absolute methanol and dried over anhydrous magnesium. $DMSO_2$ was analyzed by gas chromatography/mass spectrometry (GC-MS, MS: Agilent 5973i; GC: Agilent 6890 N equipped with an OV1701 capillary column 30 m × 0.25 mm × 0.25 μm). Analysis conditions were as follows: injection volume: 1 μl and column temperature: heating from 100 to 265°C at 30°C min^{-1}.

Results

Characterization

The analyzed FePc content is shown in Fig. S1. Its concentration was 0.0222 g/L or 1.4×10^{-4} mol/g.

Thermal Gravimetric Analyzer (TGA/DSC1/1100LF, Mettler, USA) was used to investigate the thermal properties of the materials. The pyrolysis temperature of FePc-P4VP/PET, PET/P4VP, PET, and FePc/PET was determined. As shown in Fig. S2, FePc-P4VP/PET decomposition begins at 300 °C lower than PET/P4VP, PET, and FePc/PET, but it can be used normally during the degradation experiment.

As shown in Fig. 1, the UV-vis spectrum of FePc contains a characteristic Q-band in the near-infrared region centered at 635 nm (Kay et al. 2005), a B-band at 329 nm and a weaker transition at ~ 565 nm. The characteristic Q-band is attributed to a $\pi - \pi^*$ transition from the highest occupied molecular orbital (HOMO) to the lowest unoccupied molecular orbital (LUMO) of the FePc ring. The B-band is caused by transitions between a2u and b1u to eg* orbitals, and the additional weak vibrational satellite band at ~ 565 nm is observed as a result of the inevitable aggregation between the FePc units (Kay et al. 2005; van Doorslaer et al. 2012). Compared with FePc-P4VP/PET and FePc, the characteristic Q-band for FePc-P4VP/PET

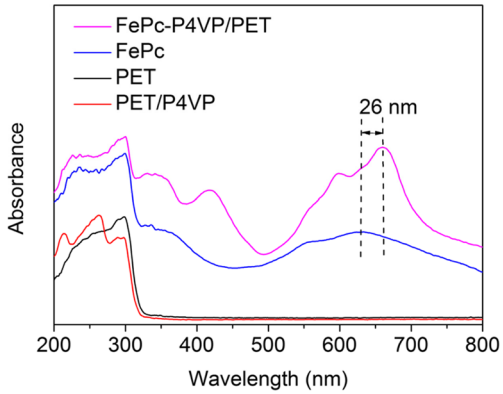

Fig. 1 UV-visible absorption spectra of FePc-P4VP/PET, FePc, P4VP/PET NFs, and PET NFs

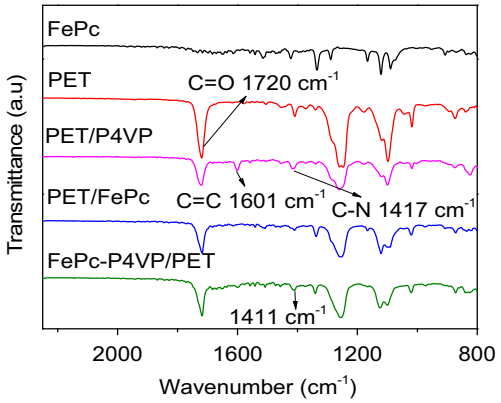

Fig. 2 ATR-FTIR spectra of FePc, FePc-P4VP/PET, FePc/PET NFs, P4VP/PET NFs, and PET NFs

exhibits a significant red shift of 662 nm from FePc (635 nm). This can be explained as the metallic iron of FePc reacting with nitrogen atoms of P4VP; nitrogen atoms provide electrons to metallic iron and the energy gap narrows between the HOMO and the LUMO of the FePc ring (Liu et al. 2008).

As shown in Fig. 2, the ATR-FTIR spectra show characteristic peaks of the skeleton stretching of FePc at ~ 1099, 1050, and 823 cm^{-1} and C-C and C-N of P4VP at ~ 1601 and 1417 cm^{-1}, respectively (Sahiner and Yasar 2013, 2014, 2015; Gashti et al. 2015). A comparison of FePc-P4VP/PET with PET/P4VP shows some new peaks at ~ 1340, 1250, and 1125 cm^{-1}, which are characteristic peaks of FePc. This proves that FePc exists in FePc-P4VP/PET. However, another peak appeared at 1411 cm^{-1}, which can be explained from P4VP reacting with FePc; the C-N peak position shifted as was confirmed by UV-vis diffuse reflectance (Lambda 900, Perkin Elmer, USA).

XPS was used to investigate the chemical composition and bonding between FePc and P4VP. As shown in Fig. S3, spectra from a wide scan showed that a new band of nitrogen was detected when FePc and P4VP were supported on PET NFs. The spectra from a wide scan also showed that a new band of iron was detected after FePc reacted with PET/P4VP, which suggests that FePc was supported on PET/P4VP NFs. The full half-widths of the N1 peaks in Fig. 3 show a typical peak of N1 in Fig. 3b–e and no typical peak of N in Fig. 3a. No elemental N exists in the PET NFs, so no typical N peak is present in PET NFs. The N1 peaks were 398.69, 397.82, and 397.91 eV as shown in Fig. 3b–d, respectively (Agboola and Ozoemena 2008), which proves that the N1 peaks of FePc and P4VP were 397.91–398.69 and 397.82 eV, respectively. Four N1 peaks exist in Fig. 3e 399.18, 398.70, 398.11, and 397.80 eV. Three new peaks emerged at 399.18, 398.11, and 397.80 eV, and the peak of the PET/P4VP NFs decreased. This behavior can be explained as nitrogen-containing groups of PET/P4VP NFs reacting with FePc and the formation of Fe-N. The peak area ratio of 399.18, 398.11, and 397.80 eV was 1:4:4, which can be explained as the nitrogen atoms of PET/P4VP, aza-bridging and pyrrole of FePc ring after PET/P4VP NFs reacting with FePc. This result provides further evidence that nitrogen atoms can coordinate axially with iron phthalocyanine in the center of metallic iron, which agrees with the UV-vis diffuse reflectance and FTIR analysis.

Degradation experiment

Oxidative degradation of SQX

To investigate the catalytic activity of FePc-P4VP/PET film, we selected SQX in aqueous solution (0.02 mM) as the substrate for the catalytic oxidation. As shown in Fig. 4, SQX decreased by 5, 6, and 58% with FePc-P4VP/PET and PET and P4VP mass ratios of 10:1, 5:1, and 1:1, respectively, and without H_2O_2 for 120 min at 50 °C, and the adsorption process reached equilibrium. When SQX in aqueous solution was exposed to FePc-P4VP/PET film and H_2O_2, the catalyst removed 12, 30, and more than 95% of the SQX for a PET and P4VP mass ratio of 10:1, 5:1, and 1:1, respectively. By comparing the catalytic degradation of SQX by the catalyst with different mass ratios of PET and P4VP in the presence or absence of H_2O_2, we concluded that the catalytic property of the catalyst with the mass ratio of PET to P4VP is 1:1 is best. Therefore, we chose the catalyst with a PET and P4VP mass ratio of 1:1 in the experiments to study the effect of the influencing factors on the catalytic degradation of SQX. In order to prove the conclusions from the experimental data are proper, we have done a series of repetition tests and got the standard deviation curve as shown in the Fig. S4. Therefore, this graph proves that the experiments carried out in this study have good repeatability, and the conclusions are convincing.

Effect of hydrogen peroxide concentration

Hydrogen peroxide as the oxidant is an important factor that affects the catalytic process. Figure S5 shows the

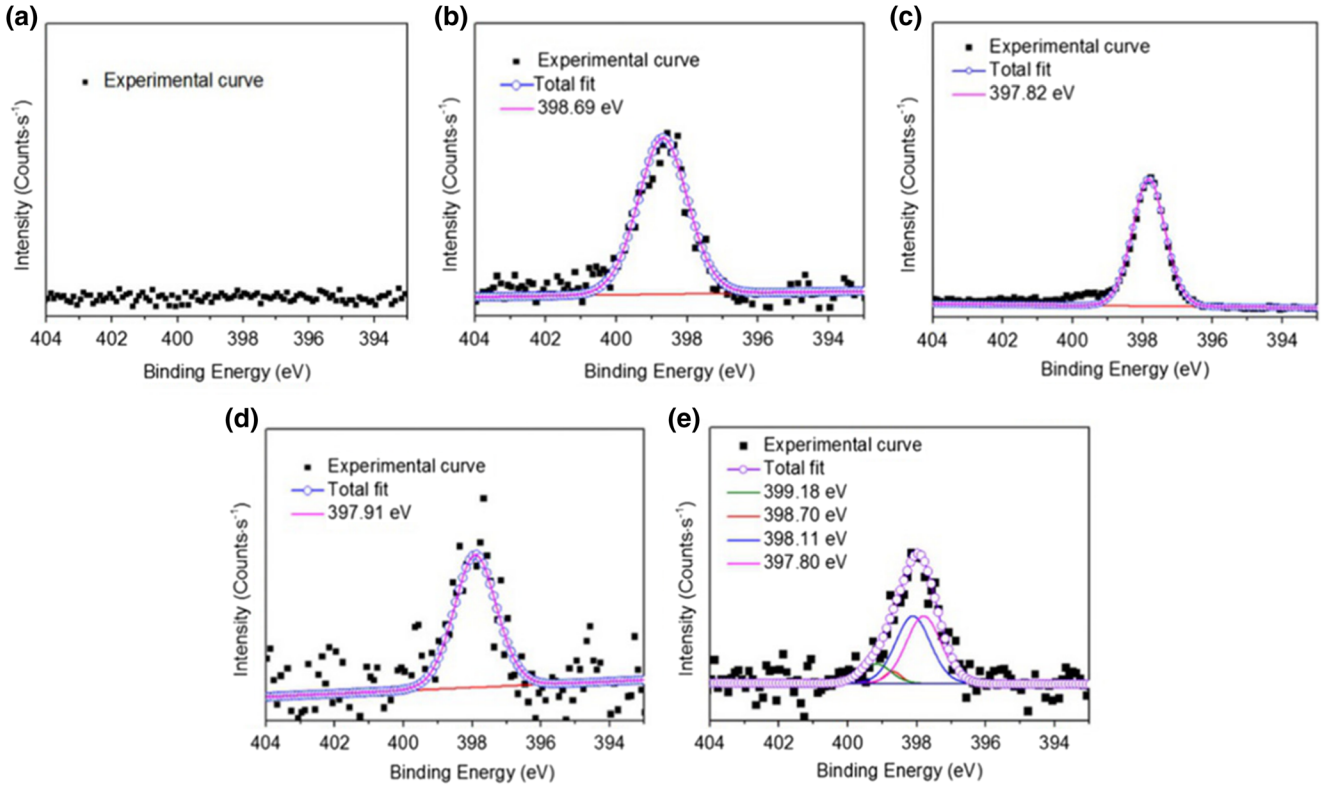

Fig. 3 XPS spectra of **a** PET NFs, **b** P4VP/PET NFs, **c** FePc, **d** FePc/PET NFs, and **e** FePc-P4VP/PET (a color version of this figure can be viewed online)

concentration of hydrogen peroxide from 5 to 20 mM; a greater hydrogen peroxide concentration results in an increased degradation rate of SQX. However, the degradation rate of SQX shows almost no difference after 120 min at 50 °C for a concentration of hydrogen peroxide of 10–20 mM. To improve the utilization of hydrogen peroxide, the experimental hydrogen peroxide concentration was selected at 10 mM.

Effect of pH

Wastewater has a certain pH range, and therefore, a study on catalyst adsorption or substrate degradation under different pH conditions is necessary. As shown in Fig. S6a, without H_2O_2, the adsorption rates were 97, 61, and 54% at a pH of 3, 7, and 9, respectively, after 120 min at 50 °C, which indicates that the adsorption capability of FePc-P4VP/PET to SQX decreased with the increase of pH. This is because the transformation of the electronegativity of SQX under the different pH values. As shown in Fig. S6b, with H_2O_2, the degradation rates of SQX achieved 100.0, 95.2, and 78.1%. A small, gradual increase in amount of SQX in solution resulted with an increase in pH. Fig. S6a and Fig. S6b show that a greater adsorption yields a greater degradation rate. We believe that the high adsorption capability of FePc-P4VP/PET could improve the degradation rate of SQX.

Effect of temperature

We also investigated the effect of temperature on SQX degradation. As shown in Fig. S7, FePc-P4VP/PET can degrade SQX from 35 to 65 °C, although the degradation rates of SQX increased with increasing temperature. The reason behind this is that the higher the temperature, the faster the motion of molecules in the system. So, we can obtain higher probability of catalyst contact with substrate. Moreover, the

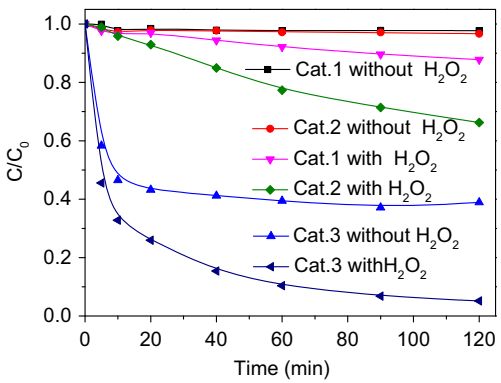

Fig. 4 Concentration changes of SQX under different conditions. [Cat:FePc-P4VP/PET] = 2 g/L, m(P4VP):m(PET) = 1:10 in Cat.1, m(P4VP):m(PET) = 1:5 in Cat.2, m(P4VP):m(PET) = 1:1 in Cat.3, [SQX] = 0.02 mM, [H_2O_2] = 10 mM; T = 50 °C, pH 7

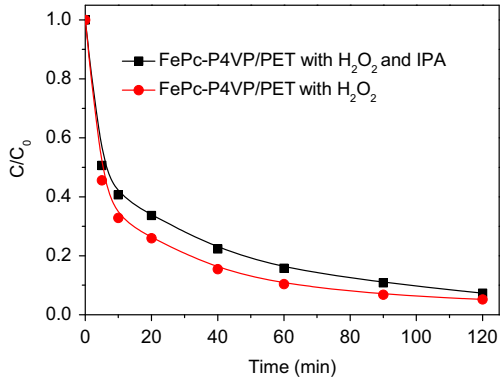

Fig. 5 Influence of IPA on SQX degradation. [FePc-P4VP/PET] = 2 g/L, [SQX] = 0.02 mM, [H_2O_2] = 10 mM, [IPA] = 0.04 M; T = 50 °C, pH 7

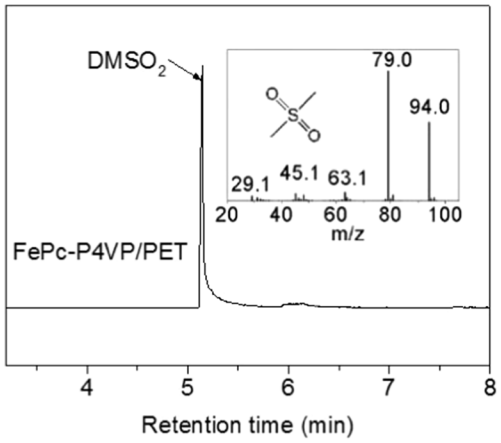

Fig. 7 GC-MS chromatograms of $DMSO_2$ (1 mM), oxidation products of DMSO catalyzed by FePc-P4VP/PET (2 g/L). The inset shows the MS spectrum of $DMSO_2$

difference in residual SQX at 50 and 65 °C was small. To conserve energy, we selected 50 °C in the experiment.

Degradation of other sulfonamides

Table S1 shows the degradation results of seven other kinds of sulfonamides by the FePc-P4VP/PET and H_2O_2 system. The seven SAs were sulfadoxine (SGD), sulfadiazine (SD), sulfamethazine (SMZ), sulfamethoxydiazine (SMD), suladimethoxypyrimidine (SMM), sulfa-chloro pyridazine (SCP), and sulfamethoxazole (SMX). The difference in degradation ability between the FePc-P4VP/PET and the H_2O_2 system was small compared with the seven SAs, which can be degraded over a certain period of time.

Investigation of active species

IPA is a good ·OH scavenger and has been used to capture reactive species during catalytic reactions (van Doorslaer et al. 2012). SQX degradation on FePc-P4VP/PET in the presence of H_2O_2 with or without IPA is shown in Fig. 5. The SQX transformation was inhibited slightly by excess IPA. Therefore, ·OH may not play a dominant role in SQX degradation.

EPR spin trapping was used to study the ·OH mentioned above. Typical 1:2:2:1 spectra, which are indicative of the DMPO − OH spin adduct (Nawrot et al. 2009; Gehling et al. 2014), indicate the formation of ·OH. In various Fenton/Fenton-like catalyst systems, the formation of ·OOH is accompanied by ·OH. The EPR spin trap technique (with DMPO) was used to probe the possible reactive oxygen species. Figure 6a shows typical EPR signals of DMPO-OH in the reaction of FePc-P4VP/PET with H_2O_2 at pH 3, 7, and 9. The formation of ·OOH radicals was also detected in methanol (Fig. 6b) because ·OOH radicals in water are unstable and undergo facile disproportionation rather than slow reaction with DMPO. The EPR signal at pH 3 is more obvious than for the other two groups. However, the typical EPR signals at pH 3, 7, and 9 were not very strong. This verified that ·OH and ·OOH were ineffective reactive species for SQX degradation.

Sulfoxides (e.g., dimethyl sulfoxide, methyl phenyl sulfoxide, and methyl p-tolyl sulfoxide) can react with Fe(IV) = O through a two-electron transfer step to produce corresponding sulfones; however, ·OH will produce a different product under the same conditions (Tai et al. 2004; Gao et al. 2012). As shown in Fig. 7, the peak of a standard sample of $DMSO_2$ (5.28 min) emerged in the FePc-P4VP/PET/H_2O_2 system. We

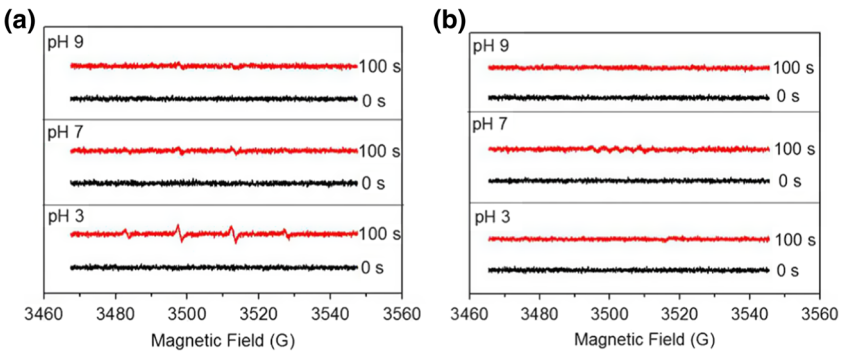

Fig. 6 DMPO spin trapping EPR spectra in aqueous **a** or methanol **b** solution in the presence of FePc-P4VP/PET film and H_2O_2 (10 mM) with DMPO (10 mM); T = 50 °C, pH 7

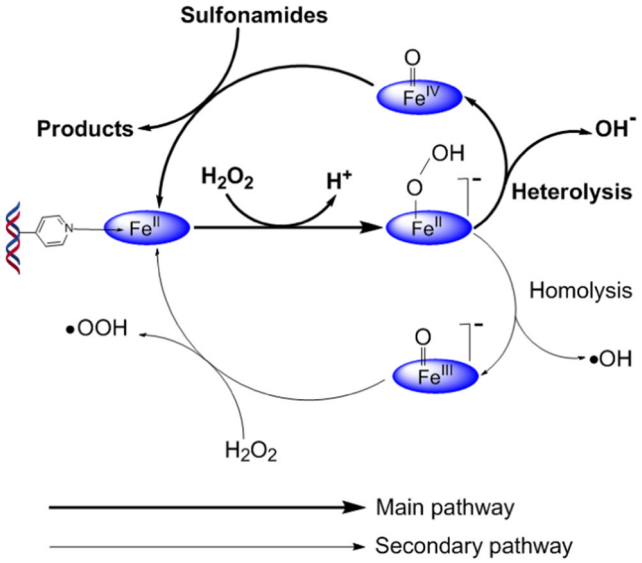

Scheme 2 Catalytic mechanism of degradation experiment

infer that the FePc-P4VP/PET/H_2O_2 system produced active Fe(IV) = O species during the degradation experiment.

Catalytic mechanism

Previous literature has indicated that the homolytic and heterolytic cleavage of the O-O bond competes when H_2O_2 is activated by MPcs (Boreen et al. 2005; Sorokin 2013; Ikhlaq et al. 2013) and that catalytic active species such as ·OH, ·OOH, and Fe(IV) = O are generated (Afanasiev and Sorokin 2016). As shown in Scheme 2, two possible pathways for the formation of catalytically active species were proposed. In the catalytic system, the heterolysis of the O-O bond was dominant in the decomposition of H_2O_2 owing to P4VP as an electron donor that could offer the electron can be a boost for the heterolysis of the O-O bond, resulting in the formation of Fe(IV) = O species (Scheme 2).

Conclusions

This study proves the significant catalytic activity of FePc-P4VP/PET, in which FePc and P4VP/PET nanofibers produced by electrospinning were used as axial ligands. The mechanism was explained and the intermediates of SQX were ·OH, ·OOH, and Fe(IV) = O using this catalyst. Less ·OH and ·OOH formed in the FePc-P4VP/PET/H_2O_2 system, more active species of Fe(IV) = O participate in the catalytic degradation of SQX. These active species were determined by classical quenching tests with IPA. EPR tests were conducted with DMPO as spin trapping agent, and Fe(IV) = O active species were detected as reaction products from DMSO.

Funding information This work was supported by the National Natural Science Foundation of China (No. 51703201) and Zhejiang Provincial Natural Science Foundation of China (No. LQ17E030003).

References

Afanasiev P, Sorokin AB (2016) μ-Nitrido diiron macrocyclic platform: particular structure for particular catalysis. Acc Chem Res 49(4): 583–593. https://doi.org/10.1021/acs.accounts.5b00458

Agboola BO, Ozoemena KI (2008) Self-assembly and heterogeneous electron transfer properties of metallo-octacarboxyphthalocyanine complexes on gold electrode. Phys Chem Chem Phys 10(17): 2399–2408. https://doi.org/10.1039/b800611c

Baran W, Adamek E, Ziemiańska J, Sobczak A (2011) Effects of the presence of sulfonamides in the environment and their influence on human health. J Hazard Mater 196:1–15. https://doi.org/10.1016/j.jhazmat.2011.08.082

Ben W, Shi Y, Li W, Zhang Y, Qiang Z (2017) Oxidation of sulfonamide antibiotics by chlorine dioxide in water: kinetics and reaction pathways. Chem Eng J 327:743–750. https://doi.org/10.1016/j.cej.2017.06.157

Bialk-Bielińska A, Stolte S, Arning J, Uebers U, Böschen A, Stepnowski P, Matzke M (2011) Ecotoxicity evaluation of selected sulfonamides. Chemosphere 85(6):928–933. https://doi.org/10.1016/j.chemosphere.2011.06.058

Biošić M, Mitrevski M, Babic S (2017) Environmental behavior of sulfadiazine, sulfamethazine, and their metabolites. Environ Sci Pollut Res 24(10):9802–9812. https://doi.org/10.1007/s11356-017-8639-8

Bloem E, Albihn A, Elving J, Hermann L, Lehmann L, Sarvi M, Schaaf T, Schick J, Turtola E, Ylivainio K (2017) Contamination of organic nutrient sources with potentially toxic elements, antibiotics and pathogen microorganisms in relation to P fertilizer potential and treatment options for the production of sustainable fertilizers: a review. Sci Total Environ 607:225–242. https://doi.org/10.1016/j.scitotenv.2017.06.274

Boreen AL, Arnold WA, Mcneill K (2005) Triplet-sensitized photodegradation of sulfa drugs containing six-membered heterocyclic groups : identification of an SO_2 extrusion photoproduct. Environ Sci Technol 39(10):3630–3638. https://doi.org/10.1021/es048331p

Carmona E, Andreu V, Pico Y (2014) Occurrence of acidic pharmaceuticals and personal care products in Turia River Basin: from waste to drinking water. Sci Total Environ 484:53–63. https://doi.org/10.1016/j.scitotenv.2014.02.085

Cetecioglu Z (2014) Aerobic inhibition assessment for anaerobic treatment effluent of antibiotic production wastewater. Environ Sci Pollut Res 21(4):2856–2864. https://doi.org/10.1007/s11356-013-2243-3

Dewil R, Mantzavinos D, Poulios I, Rodrigo MA (2017) New perspectives for advanced oxidation processes. J Environ Manag 195(Pt 2): 93–99. https://doi.org/10.1016/j.jenvman.2017.04.010

Gao Y-Q, Gao N-Y, Deng Y, Yang Y-Q, Ma Y (2012) Ultraviolet (UV) light-activated persulfate oxidation of sulfamethazine in water. Chem Eng J 195-196:248–253. https://doi.org/10.1016/j.cej.2012.04.084

Gashti MP, Ebrahimi I, Pousti M (2015) New insights into corona discharge surface ionization of polyethylene terephthalate via a combined computational and experimental assessment. Curr Appl Phys 15(9):1075–1083. https://doi.org/10.1016/j.cap.2015.06.009

Gehling W, Khachatryan L, Dellinger B (2014) Hydroxyl radical generation from environmentally persistent free radicals (EPFRs) in $PM_{2.5}$. Environ Sci Technol 48(8):4266–4272. https://doi.org/10.1021/es401770y

González O, Justo A, Bacardit J, Ferrero E, Malfeito JJ, Sans C (2013) Characterization and fate of effluent organic matter treated with UV/H_2O_2 and ozonation. Chem Eng J 226:402–408. https://doi.org/10.1016/j.cej.2013.04.066

Guo Z, Zhou F, Zhao Y, Zhang C, Liu F, Bao C (2012a) Gamma irradiation-induced sulfadiazine degradation and its removal mechanisms. Chem Eng J 191:256–262. https://doi.org/10.1016/j.cej.2012.03.012

Guo C, Xu J, Zhang Y, He Y (2012b) Hierarchical mesoporous TiO_2 microspheres for the enhanced photocatalytic oxidation of sulfonamides and their mechanism. RSC Adv 2(11):4720–4727. https://doi.org/10.1039/c2ra01164f

Hoff RB, Barreto F, Kist TBL (2009) Use of capillary electrophoresis with laser-induced fluorescence detection to screen and liquid chromatography-tandem mass spectrometry to confirm sulfonamide residues: validation according to European Union 2002/657/EC. J Chromatogr A 1216(46):8254–8261. https://doi.org/10.1016/j.chroma.2009.07.074

Hoff RB, Barreto F, Melo J, Jank L, Peralba MDCR, Pizzolato TM (2012) Characterization and estimation of sulfaquinoxaline metabolites in animal tissues using liquid chromatography coupled to tandem mass spectrometry. Anal Methods 4(9):2822. https://doi.org/10.1039/C2AY25197C

Hoff RB, Meneghini L, Pizzolato TM, Peralba MDCR, Díaz-Cruz MS, Barceló D (2014) Structural elucidation of sulfaquinoxaline metabolism products and their occurrence in biological samples using high-resolution Orbitrap mass spectrometry. Anal Chem 86(11):5579–5586. https://doi.org/10.1021/ac501132r

Hou J, Wang C, Mao D, Luo Y (2016) The occurrence and fate of tetracyclines in two pharmaceutical wastewater treatment plants of Northern China. Environ Sci Pollut Res 23(2):1722–1731. https://doi.org/10.1007/s11356-015-5431-5

Ikhlaq A, Brown DR, Kasprzyk-Hordern B (2013) Mechanisms of catalytic ozonation: an investigation into superoxide ion radical and hydrogen peroxide formation during catalytic ozonation on alumina and zeolites in water. Appl Catal B Environ 129:437–449. https://doi.org/10.1016/j.apcatb.2012.09.038

Kay P, Blackwell PA, Boxall ABA (2005) A lysimeter experiment to investigate the leaching of veterinary antibiotics through a clay soil and comparison with field data. Environ Pollut 134(2):333–341. https://doi.org/10.1016/j.envpol.2004.07.021

Kovacic M, Perisic DJ, Biosic M, Kusic H, Babic S, Bozic AL (2016) UV photolysis of diclofenac in water; kinetics, degradation pathway and environmental aspects. Environ Sci Pollut Res 23(15):14908–14917. https://doi.org/10.1007/s11356-016-6580-x

Lekunberri I, Villagrasa M, Luis Balcázar J, Borrego CM (2017) Contribution of bacteriophage and plasmid DNA to the mobilization of antibiotic resistance genes in a river receiving treated wastewater discharges. Sci Total Environ 601:206–209. https://doi.org/10.1016/j.scitotenv.2017.05.174

Liao Q-N, Ji F, Li J-C, Zhan X, Hu Z-H (2016) Decomposition and mineralization of sulfaquinoxaline sodium during UV/H_2O_2 oxidation processes. Chem Eng J 284:494–502. https://doi.org/10.1016/j.cej.2015.08.150

Lin H, Zhang J, Chen H, Wang J, Sun W, Zhang X, Yang Y, Wang Q, Ma J (2017) Effect of temperature on sulfonamide antibiotics degradation, and on antibiotic resistance determinants and hosts in animal manures. Sci Total Environ 607:725–732. https://doi.org/10.1016/j.scitotenv.2017.07.057

Liu Y, Wang J (2013) Degradation of sulfamethazine by gamma irradiation in the presence of hydrogen peroxide. J Hazard Mater 250-251:99–105. https://doi.org/10.1016/j.jhazmat.2013.01.050

Liu J, Huang J-W, Shen H, Wang H, Yu H-C, Ji L-N (2008) The synthesis of two novel hybrids containing a zinc(II) porphyrin unit and a polypyridyl ruthenium(II) complex unit and their photoinduced intramolecular electron and energy transfer. Dyes Pigments 77(2):374–379. https://doi.org/10.1016/j.dyepig.2007.06.008

Mano T, Nishimoto S, Kameshima Y, Miyake M (2015) Water treatment efficacy of various metal oxide semiconductors for photocatalytic ozonation under UV and visible light irradiation. Chem Eng J 264:221–229. https://doi.org/10.1016/j.cej.2014.11.088

Mantzavinos D, Poulios I, Fernández-Ibañez P, Malato S (2014) Advanced oxidation processes for environmental protection. Environ Sci Pollut Res 21(21):12109–12111. https://doi.org/10.1007/s11356-014-3359-9

Mantzavinos D, Poulios I, Pintar A (2017) Advances and trends in advanced oxidation processes. Environ Sci Pollut Res 24(2):1061–1062. https://doi.org/10.1007/s11356-016-8021-2

Nawrot TS, Kuenzli N, Sunyer J, Shi T, Moreno T, Viana M, Heinrich J, Forsberg B, Kelly FJ, Sughis M, Nemery B, Borm P (2009) Oxidative properties of ambient $PM_{2.5}$ and elemental composition: heterogeneous associations in 19 European cities. Atmos Environ 43(30):4595–4602. https://doi.org/10.1016/j.atmosenv.2009.06.010

Nidheesh PV, Gandhimathi R (2014a) Comparative removal of Rhodamine B from aqueous solution by electro-Fenton and electro-Fenton-like processes. Clean Soil Air Water 42(6):779–784. https://doi.org/10.1002/clen.201300093

Nidheesh PV, Gandhimathi R (2014b) Electrolytic removal of Rhodamine B from aqueous solution by peroxicoagulation process. Environ Sci Pollut Res 21(14):8585–8594. https://doi.org/10.1007/s11356-014-2775-1

Nidheesh PV, Gandhimathi R, Ramesh ST (2013) Degradation of dyes from aqueous solution by Fenton processes: a review. Environ Sci Pollut Res 20(4):2099–2132. https://doi.org/10.1007/s11356-012-1385-z

Ou D, Chen B, Bai R, Song P, Lin H (2015) Contamination of sulfonamide antibiotics and sulfamethazine-resistant bacteria in the downstream and estuarine areas of Jiulong River in Southeast China. Environ Sci Pollut Res 22(16):12104–12113. https://doi.org/10.1007/s11356-015-4473-z

Sahiner N, Yasar AO (2013) The generation of desired functional groups on poly(4-vinyl pyridine) particles by post-modification technique for antimicrobial and environmental applications. J Colloid Interface Sci 402:327–333. https://doi.org/10.1016/j.jcis.2013.03.032

Sahiner N, Yildiz S (2014) Preparation of superporous poly(4-vinyl pyridine) cryogel and their templated metal nanoparticle composites for H_2 production via hydrolysis reactions. Fuel Process Technol 126:324–331. https://doi.org/10.1016/j.fuproc.2014.05.025

Sahiner N, Atta AM, Yasar AO, Al-Lohedan HA, Ezzat AO (2015) Surface activity of amphiphilic cationic pH-responsive poly(4-vinylpyridine) microgel at air/water interface. Colloids Surf A Physicochem Eng Asp 482:647–655. https://doi.org/10.1016/j.colsurfa.2015.07.035

Sakai N, Sakai M, Haron DEM, Yoneda M, Mohd MA (2016) Beta-agonist residues in cattle, chicken and swine livers at the wet market and the environmental impacts of wastewater from livestock farms in Selangor State, Malaysia. Chemosphere 165:183–190. https://doi.org/10.1016/j.chemosphere.2016.09.022

Salaeh S, Perisic DJ, Biosic M, Kusic H, Babic S, Stangar UL, Dionysiou DD, Bozic AL (2016) Diclofenac removal by simulated solar assisted photocatalysis using TiO_2-based zeolite catalyst; mechanisms, pathways and environmental aspects. Chem Eng J 304:289–302. https://doi.org/10.1016/j.cej.2016.06.083

Sorokin AB (2013) Phthalocyanine metal complexes in catalysis. Chem Rev 113(10):8152–8191. https://doi.org/10.1021/cr4000072

Sorokin AB, Kudrik EV (2011) Phthalocyanine metal complexes: versatile catalysts for selective oxidation and bleaching. Catal Today 159(1):37–46. https://doi.org/10.1016/j.cattod.2010.06.020

Tai C, Peng J-F, Liu J-F, Jiang G-B, Zou H (2004) Determination of hydroxyl radicals in advanced oxidation processes with dimethyl

sulfoxide trapping and liquid chromatography. Anal Chim Acta 527(1):73–80. https://doi.org/10.1016/j.aca.2004.08.019

van Doorslaer X, Heynderickx PM, Demeestere K, Debevere K, Van Langenhove H, Dewulf J (2012) TiO_2 mediated heterogeneous photocatalytic degradation of moxifloxacin: operational variables and scavenger study. Appl Catal B Environ 111-112:150–156. https://doi.org/10.1016/j.apcatb.2011.09.029

Vasiliadou IA, Molina R, Martínez F, Melero JA (2013) Biological removal of pharmaceutical and personal care products by a mixed microbial culture: sorption, desorption and biodegradation. Biochem Eng J 81: 108–119. https://doi.org/10.1016/j.bej.2013.10.010

Wang L, Wu J, Wang Q, He C, Zhou L, Wang J, Pu Q (2012) Rapid and sensitive determination of sulfonamide residues in milk and chicken muscle by microfluidic chip electrophoresis. J Agric Food Chem 60(7):1613–1618. https://doi.org/10.1021/jf2036577

Wang M, Liu X, Pan B, Zhang S (2013) Photodegradation of Acid Orange 7 in a UV/acetylacetone process. Chemosphere 93(11): 2877–2882. https://doi.org/10.1016/j.chemosphere.2013.08.082

Wang A-Q, Lin Y-L, Xu B, Hu C-Y, Xia S-J, Zhang T-Y, Chu W-H, Gao N-Y (2017) Kinetics and modeling of iodoform degradation during UV/chlorine advanced oxidation process. Chem Eng J 323:312–319. https://doi.org/10.1016/j.cej.2017.04.061

Wols BA, Harmsen DJH, Beerendonk EF, Hofman-Caris CHM (2015) Predicting pharmaceutical degradation by UV (MP)/H_2O_2 processes: a kinetic model. Chem Eng J 263:336–345. https://doi.org/10.1016/j.cej.2014.10.101

Yu Y, Liu Y, Wu L (2013) Sorption and degradation of pharmaceuticals and personal care products (PPCPs) in soils. Environ Sci Pollut Res 20(6):4261–4267. https://doi.org/10.1007/s11356-012-1442-7

Zhang Y, Xu J, Zhong Z, Guo C, Li L, He Y, Fan W, Chen Y (2013) Degradation of sulfonamides antibiotics in lake water and sediment. Environ Sci Pollut Res 20(4):2372–2380. https://doi.org/10.1007/s11356-012-1121-8

Zhao X, Wang J, Zhu L, Ge W, Wang J (2017) Environmental analysis of typical antibiotic-resistant bacteria and ARGs in farmland soil chronically fertilized with chicken manure. Sci Total Environ 593: 10–17. https://doi.org/10.1016/j.scitotenv.2017.03.062

Zhu Z, Chen Y, Gu Y, Wu F, Lu W, Xu T, Chen W (2016) Catalytic degradation of recalcitrant pollutants by Fenton-like process using polyacrylonitrile-supported iron (II) phthalocyanine nanofibers: intermediates and pathway. Water Res 93:296–305. https://doi.org/10.1016/j.watres.2016.02.035